GPT-4V Cannot Generate Radiology Reports Yet

Yuyang Jiang[*]
University of Chicago
yuyang2001@uchicago.edu

Chacha Chen[*]
University of Chicago
chacha@uchicago.edu

Dang Nguyen
University of Chicago
dangnguyen@uchicago.edu

Benjamin M. Mervak
University of Michigan
bmervak@med.umich.edu

Chenhao Tan
University of Chicago
chenhao@uchicago.edu

Abstract

GPT-4's purported strong multimodal abilities raise interests in using it to automate radiology report writing, but there lacks thorough evaluations. In this work, we perform a systematic evaluation of GPT-4 (4o and vision-preview) in generating radiology reports across three chest X-ray report benchmarks: MIMIC-CXR, CheXpert Plus, and IU X-Ray. We attempt to directly generate reports with different prompting strategies and find that the models fail terribly in both lexical metrics and clinical efficacy metrics. To understand the low performance, we decompose the task into two steps: 1) the **medical image reasoning** step of predicting medical condition labels from images; and 2) the **report synthesis** step of generating reports from (groundtruth) conditions. We show that GPT-4's performance in image reasoning is consistently low across different prompts. In fact, the distributions of model-predicted labels remain constant regardless of which groundtruth conditions are present on the image, suggesting that the model is not interpreting chest X-rays meaningfully. Even when given groundtruth conditions in report synthesis, its generated reports are less correct and less natural-sounding than a finetuned Llama. Altogether, our findings cast doubt on the viability of using GPT-4 in a radiology workflow.

1 Introduction

Large language models (LLMs) are becoming multimodal, and GPT-4 model series represent the state-of-the-art. [1] Similar to the claimed general-purpose capabilities in LLMs (Bubeck et al., 2023; Nori et al., 2023), large multimodal models are supposed to possess advanced skills across a wide range of domains, including high-stakes scenarios such as medicine (Yang et al., 2023). However, in the field of radiology report generation, where relatively rich datasets are available, there has been *inconclusive* and even *contradictory* evidence regarding the performance of LMMs. Some studies (Liu et al., 2023b; Yang et al., 2023) claimed that GPT-4V performs well to some extent based on case studies and qualitative analysis. In contrast, Brin et al. (2023) found that the model is not yet a reliable tool for radiological image interpretation on a small private dataset. Wu et al. (2023) observed that GPT-4V can generate structured reports with incorrect content, as evidenced by case studies and qualitative analysis. Moreover, existing evaluation works tend to work with either very small size of samples (Yang et al., 2023) or limited evaluation metrics (Li et al., 2023). Our work distinguishes itself by providing an in-depth evaluation and analysis on *why* GPT-4V fails at this task. [2]

To do that, we perform three experiments as shown in Fig. 1 on three main radiology report generation benchmarks: MIMIC-CXR, CheXpert Plus, and IU X-Ray. Our evaluation starts with Experiment 1: **direct report generation**. Different from previous works (Liu et al., 2023b; Yang et al., 2023), we conduct a thorough evaluation of GPT-4V's capability to directly generate reports from chest X-rays, utilizing different prompting strategies and assessing both lexical metrics, which measure how textually similar a generated report is to a reference report, and clinical efficacy metrics, which measure how clinically accurate it is. We experiment with various prompting strategies, including zero-shot, contextual enhancement, chain-of-thought (CoT) (Wei et al., 2022), and few-shot

---

[*]Equal contribution.
[1] https://huggingface.co/spaces/WildVision/vision-arena.

[2]We access GPT-4 vision model series (inlcuding gpt-4-vision-preview and gpt-4o) through Azure OpenAI service to prevent sharing data with third parties. Due to limited space, we mainly show evaluation results of GPT-4o in the main paper. Throughout the paper, we use GPT-4V to refer to GPT-4o, unless otherwise specified. Full evaluation results of GPT-4o, GPT-4-vision-preview, and the open sourced Llama3.2-90B-vision-instruct can be found in Appendix C.
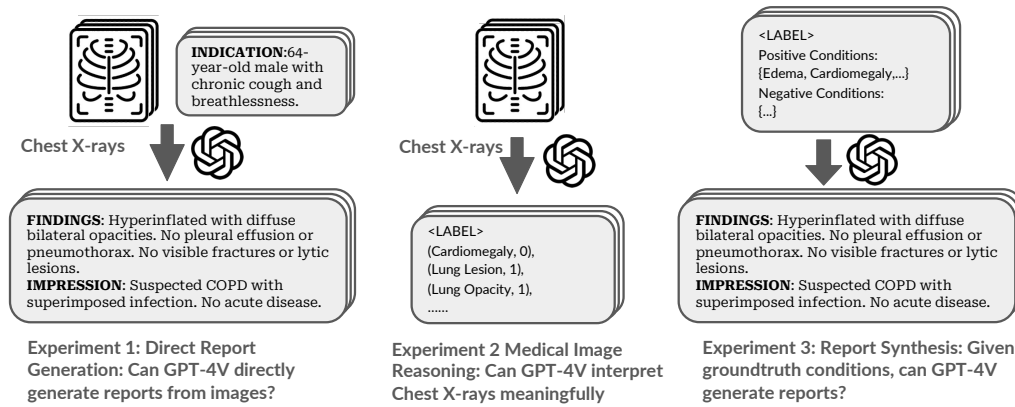
Figure 1: Evaluation overview. In Experiment 1, we evaluate the out-of-box capability of GPT-4V. We further decompose the task into medical image reasoning (Experiment 2) and report synthesis (Experiment 3).

in-context learning. Despite our various attempts, the performance of GPT-4V is consistently low in both metrics.

To further investigate the reason for GPT-4V's poor performance, we break down report generation into two steps, **medical image reasoning** and **report synthesis given medical conditions**. For Experiment 2 (medical image reasoning), we first test whether GPT-4V can identify medical conditions from X-rays. Our findings indicate that GPT-4's performance in identifying medical conditions from images is unsatisfactory across different prompts. Based on limited capability results, we further compare the difference between distributions of predicted medical condition labels conditioned on different groundtruth image labels. We find that GPT-4V cannot interpret medical images meaningfully as the distribution of predicted labels does not vary depend on the groundtruth label.

Finally, in Experiment 3 (report synthesis), we explore whether bypassing the image reasoning bottleneck by providing groundtruth conditions enables GPT-4V to generate clinically usable reports. As expected, reports generated by GPT-4V achieve higher clinical efficacy; however, the limited improvement in lexical metrics suggests that GPT-4V-generated reports remain dissimilar to human-written reports in style. Most importantly, GPT-4V underperforms a finetuned Llama-2 in both lexical metrics and clinical efficacy metrics, calling into question its utility. We further validate our findings by conducting an additional human reader study with two radiologist to evaluate the clinical viability of GPT-4V generated reports.

In summary, our key contributions and conclusions are as follows:

- We perform the first systematic and in-depth eval-

uation to benchmark GPT-4V in radiology report generation. Our main conclusion is that GPT-4V cannot generate radiology reports yet.

- To understand the poor performance, we decompose the task into medical image reasoning and report synthesis. We find that GPT-4V cannot interpret chest X-ray images meaningfully in the image reasoning step, and further validate this finding through rigorous hypothesis testing.

- During report synthesis, we address the image reasoning bottleneck by providing groundtruth conditions. Nonetheless, both experimental results and human evaluations consistently show that GPT-4V performs worse than a finetuned Llama-2 baseline.

2 Related Work

While there is an emerging line of work in investigating the direct application of GPT-4[3] in radiology report generation, there lacks a systematic evaluation. (Liu et al., 2023b; Wu et al., 2023; Yang et al., 2023) tested capabilities for general medical applications through case studies, including selected examples of chest X-ray reports with qualitative analysis. (Brin et al., 2023) provided quantitative results on GPT-4V's accuracy in interpreting medical images, using a small private dataset that includes chest X-rays. But their evaluation only focused on identifying the imaging modality (e.g. CT, ultrasound, or MRI) and the anatomical region of the pathology, rather than assessing the overall quality of generated radiology reports. (Li et al., 2023) evaluated GPT-4V on the public MIMIC-CXR dataset, but only used lexical

---

[3]GPT-4V mentioned in previous literature typically refers to GPT-4-vision-preview.

and semantic metrics without assessing clinical efficacy. (Chaves et al., 2024) included GPT-4V as one of the baselines. However, their focus is on proposing a new model. In contrast, we provide an in-depth evaluation across various metrics with different prompting strategies on two public datasets.

Prior work has also examined text-only applications of GPT-4 related to radiology report generation, such as summarizing findings (Liu et al., 2024b; Sun et al., 2023), handling various text processing tasks including sentence semantics, structural extraction, and summary of findings (Liu et al., 2023a), radiology board-style exams (Bhayana et al., 2023), detecting errors in radiology reports (Gertz et al., 2024), and refining human-written reports for better standardization and clarity (Hasani et al., 2023). Additionally, other related multimodal tasks include visual question answering based on radiology images (Yan et al., 2023) and biomedical image classification (Liu et al., 2023b).

To the best of our knowledge, our work provides the first systematic and in-depth evaluation of GPT-4V's capabilities to generate radiology reports.

3 Experimental Setup

Method. In Experiment 1 (Section 4.1), we evaluate GPT-4V's ability to directly generate radiology report given chest X-ray images. We consider five variations of prompts as outlined in Table 1. Prompt 1.1 (Basic generation) is a prompt to test the out-of-the-box capability of GPT-4V. We implement three additional prompting strategies leveraging insights in prompt engineering: (1) inspired by (Nguyen et al., 2023), we add relevant contextual information (i.e., the INDICATION) to derive Prompt 1.2 as "Indication enhancement", and add instructions on medical condition labels to Prompt 1.3 as "+instruction" enhancement; (2) we use a chain-of-thought (CoT) strategy in Prompt 1.4, eliciting the model with two steps: medical condition label prediction based on images followed by report synthesis based on the predicted labels; (3) We adopt few-shot in-context learning by adding a few example image-report pairs in Prompt 1.5. We compare these results with the state-of-the-art (SOTA) models.

In addition to evaluation of the end-to-end radiology report generation capability, we further evaluate on the decomposed tasks: Experiment 2 (Section 4.2): chest X-ray image reasoning; and Experiment 3 (Section 4.2): synthesizing a radiology report from given conditions. This decomposition allows us to look into the bottlenecks in the current generation performance. In Experiment 2, we prompt the model to directly output medical condition labels from images (Prompt 2.1). In Experiment 3, we bypass image reasoning to test GPT-4V's textual synthesis ability and provide groundtruth conditions to evaluate the model's report composition capability independently (Prompt 3.1). To contextualize the performance of GPT-4V, we also report the performance of a finetuned Llama-2-7B on groundtruth labels and groundtruth impressions following Alpaca (Taori et al., 2023).

Dataset and pre-processing. We use three chest X-ray datasets: MIMIC-CXR, IU X-ray and CheXpert Plus. The MIMIC-CXR dataset (Johnson et al., 2019) contains chest X-ray images and their corresponding free-text radiology reports. The dataset includes 377,110 images from 227,835 studies. Each study has one radiology report and one or more chest X-rays. The IU X-raydataset (Demner-Fushman et al., 2016) (also known as "Open-i") includes 3996 de-identified radiology reports and 8121 associated images from the Indiana University hospital network. CheXpert Plus dataset (Chambon et al., 2024) is a newly-released and comprehensive radiology data collection, featuring a total of 223,462 unique pairs of radiology reports and chest X-rays across 187,711 studies from 64,725 patients. For our evaluation, we use the whole validation set of CheXpert Plus (200 samples) and randomly sample 300 studies from each of the MIMIC-CXR and IU X-RAY datasets after removing studies with empty impression or indication sections. This results in a total of 800 samples. More details about data processing can be checked in Appendix B.

Evaluation metrics. We evaluate the generated reports from two aspects:

- Lexical metrics. Lexical metrics focus on the surface form and the exact word matches between the generated and reference texts. We adopt common lexical metrics: BLEU (Papineni et al., 2002) (1-gram and 4-gram), ROUGE-L (Lin, 2004), and METEOR (Banerjee and Lavie, 2005).

- Clinical efficacy metrics. We first evaluate on **clinical correctness** based on labeler results on generated reports. Following existing works (Hyland et al., 2023; Tu et al., 2024;

Experiment 1: Direct Report Generation	
Prompt 1.1 Basic generation	Direct report generation based on chest X-ray images
Prompt 1.2 +Indication	Contextual enhancement by providing the indication section
Prompt 1.3 +Instruction	Contextual enhancement by providing instructions on medical conditions
Prompt 1.4 Chain-of-Thought (CoT)	Step 1 - medical condition labeling; Step 2 - report synthesis
Prompt 1.5 Few-shot	Few-shot: in-context learning given a few examples
Experiment 2: Medical Image Reasoning Capability	
Prompt 2.1 Image reasoning	Medical condition labeling directly from chest X-ray images
Experiment 3: Report Synthesis Given Medical Conditions	
Prompt 3.1 Report synthesis	Report generation using provided positive and negative conditions

Table 1: An index to prompts used in all of our experiments.

Nguyen et al., 2023), we use the CheXbert automatic labeler (Smit et al., 2020) to extract labels for each of 14 Chexpert medical conditions (Irvin et al., 2019). We compute both positive F1 and negative F1, where each condition has four labels: `present, absent, uncertain, unmentioned`. Positive F1 considers only positive labels against all others, while negative F1 considers negative labels as 1 and all other labels as 0. We report the macro-averaged F1 on all 14 conditions and on top 5 conditions (which only reports on the five most common conditions[4]). We also report Rad-Graph F1 (Jain et al., 2021), which captures the overlap in clinical entities and relations between a generated report and a reference report.

Additionally, from a **pragmatic** viewpoint, commenting on negative observations is essential in radiology reports. Following Nguyen et al. (2023), we compute Negative F1 and Negative F1-5, to evaluate whether the model can accurately identify negative conditions and include that in the generated reports. All F1 scores are macro-averaged. We also use the **hallucination** metric to quantify the proportion of uninferable information. Following Nguyen et al. (2023), we define uninferable information to include previous studies, previous treatment details, recommendations, doctor communications, and image view descriptions.

4 Results

4.1 Experiment 1: Can GPT-4V directly generate reports from images?

We first evaluate the out-of-the-box capability of GPT-4V in generating radiology reports from chest

X-ray images using basic generation (Prompt 1.1). Table 2 shows the results compared with existing state-of-the-art (SOTA) models. Overall, GPT-4V significantly underperforms the state-of-the-art models on both lexical and clinical efficacy metrics, with the exception of the METEOR score on the IU X-RAY dataset. The relatively better METEOR performance is due to its comprehensive evaluation criteria, which include synonymy and paraphrasing, not just exact word matches like BLEU and ROUGE. This allows METEOR to recognize semantic equivalents, even if the word choice differs. In other words, the generated report somewhat resembles a radiology report, although it fails at the exact word-level matching. For clinical efficacy metrics, the gaps to SOTA are consistently large. This suggests that GPT-4V struggles to accurately identify conditions in its generated reports from images alone.

Our results are consistent across prompting strategies. Our prompting strategies include adding contextual information, chain-of-thought reasoning, and few-shot prompting. While indication enhancement (Prompt 1.2) provides indication section as input in addition to chest X-rays and improves many metrics for both MIMIC-CXR and IU X-RAY, it remains within the same range and does not significantly reduce the gap compared to SOTA. Instruction enhancement (Prompt 1.3) provides medical condition descriptions and makes a moderate yet still limited difference to SOTA in Positive F1 scores and Hallucination. Following the same labeling instructions, Chain-of-Thought (Prompt 1.4) similarly increases Positive F1-5 by 11.9% in MIMIC-CXR, 11.6% in IU X-RAY and 14.8% in CheXpert Plus, marking the most effective advances so far. However, it still faces a

---
[4]Top five conditions are Pneumothorax, Pneumonia, Edema, Pleural Effusion, and Consolidation.

Experiment	Lexical metrics				Clinical Efficacy Metrics					
	BLEU-1	**BLEU-4**	**ROUGE**	**METEOR**	**Pos F1**	**Pos F1@5**	**Rad. F1**	**Neg F1**[*]	**Neg F1@5**[*]	**Hall.**[*]↓
					MIMIC-CXR					
Basic	0.331	0.031	0.225	0.282	0.134	0.153	0.163	0.038	0.081	0.587
+Indication	0.333	0.044	0.234	0.290	**0.273**	0.255	0.182	**0.048**	**0.126**	0.547
+Instruction	0.276	0.028	0.203	0.264	0.155	0.230	0.154	0.042	0.101	**0.359**
CoT	0.242	0.017	0.186	0.201	0.172	**0.272**	0.119	0.008	0.020	0.397
Few-shot	**0.337**	**0.055**	**0.257**	**0.301**	0.170	0.203	**0.188**	0.035	0.091	0.477
Llama-3.2[1]	0.258	0.026	0.249	0.216	0.172	0.300	0.144	0.045	0.117	0.049
SOTA	0.402	0.142	0.291	0.333	0.473	0.516	0.267	0.077	0.156	0.158
[ref.]	Liu et al.	Hyland et al.	Liu et al.	Hyland et al.	Liu et al.	Tu et al.	Tu et al.	Nguyen et al.	Nguyen et al.	Nguyen et al.
Δ(to SOTA)	-16.17%	-61.27%	-11.68%	-9.61%	-42.28%	-47.29%	-29.59%	-37.66%	-19.23%	20.10%
					IU X-RAY					
Basic	0.316	0.045	0.238	0.311	0.059	0.045	0.203	0.000	0.000	0.303
+Indication	**0.330**	**0.049**	0.242	**0.323**	0.077	0.098	**0.214**	**0.071**	**0.051**	0.307
+Instruction	0.238	0.030	0.207	0.283	**0.081**	0.146	0.174	0.000	0.000	**0.177**
CoT	0.239	0.024	0.194	0.231	0.077	**0.161**	0.144	0.000	0.000	0.197
Few-Shot	0.279	0.044	**0.243**	0.250	0.037	0.031	0.187	0.010	0.025	0.211
Llama-3.2	0.248	0.027	0.239	0.231	0.104	0.214	0.158	0.015	0.040	0.011
SOTA	0.499	0.184	0.390	0.208	-	-	-	-	-	-
[ref.]	Liu et al.	Liu et al.	Liu et al.	Liu et al.						
Δ(to SOTA)	-36.27%	-75.82%	-38.72%	+49.52%	-	-	-	-	-	-
					CHEXPERT PLUS					
Basic	**0.237**	**0.015**	**0.176**	**0.191**	0.228	0.191	**0.112**	0.013	0.035	0.680
+Instruction	0.191	0.007	0.159	0.172	0.210	0.325	0.101	0.042	0.085	0.377
CoT	0.166	0.011	0.155	0.139	**0.234**	**0.339**	0.077	0.000	0.000	0.400
Few-shot	0.171	0.007	0.158	0.149	0.188	0.224	0.094	**0.043**	**0.111**	**0.370**
Llama-3.2	0.166	0.006	0.175	0.147	0.261	0.355	0.092	0.031	0.081	0.058
SOTA	-	0.069	0.279	-	0.366	0.495	0.285	-	-	-
[ref.]		Chambon et al.				Chambon et al.				
Δ(to SOTA)	-	-78.26%	-36.92%	-	-36.07%	-31.52%	-60.70%	-	-	-

[*] To compare with SOTA numbers, all metrics, except for those marked with [*] (Neg F1, Neg F1@5, and Hall), are evaluated on the findings section. [*] columns are based on the impression section.

CheXpert Plus doesn't have indication section in reports, thus we skip experiment with +Indication prompt.

[1] Due to the space limit, we only show the best results of prompt 1.1-1.5 for Llama-3.2-90B-Vision-Instruct. It is noted that the low hallucination rate is likely because it only outputs medical conditions (mostly wrong but not uninferable).

Full details of the performance of GPT-4o, GPT-4-vision-preview, and Llama3.2-90B-Vision-Instruct, including results for both the findings and impression sections, are provided in the Appendix C.

Table 2: Direct report generation performance comparison. GPT-4V shows a significant performance gap compared to SOTA, and the results are consistent across the five prompting strategies. Open sourced Llama3.2 performs similarly compared with GPT-4V. Examples of generated reports across different prompts can be found in Appendix C.5.

substantial gap to SOTA, with 47.29% in MIMIC-CXR and 31.52% in CheXpert Plus. Few-Shot (Prompt 1.5) provides image-report pairs as context and generally improves lexical metrics, RadGraph F1, and Hallucination, while clinical correctness, particularly in identifying positive conditions, remains consistently low across three datasets. This indicates that while few-shot prompting might help GPT-4V mimic the format of groundtruth reports, it still falls short in generating accurate reports.

4.2 Experiment 2: Can GPT-4V interpret chest X-rays meaningfully?

In this section, we probe GPT-4V's ability to reason about chest X-ray images alone. Specifically,

Metric	Chain-of-Thought (1st Step)	Image Reasoning
Positive F1	0.195	0.161
Positive F1@5	0.298	0.242

Table 3: Image reasoning performance of GPT-4V on MIMIC-CXR. The model performs poorly in identifying medical conditions from chest X-ray images.

we evaluate whether the model can meaningfully interpret chest X-ray images by measuring how accurately GPT-4V can label medical conditions present (positive F1). Table 3 provides an overview of GPT-4V's labeling performance under different prompting strategies.

We can see that GPT-4V cannot accurately specify positive conditions from given chest X-rays.

This can be highlighted by consistently poor Positive F1 scores observed from various prompting strategies. Furthermore, this inability to accurately interpret images may directly contribute to GPT-4V's failure in generating high-quality reports, as supported by similar Positive F1 score of 0.172 and Positive F1-5 score of 0.272 from the report synthesis phase of Chain-of-Thought (see Table 2), compared to 0.195 (Positive F1) and 0.298 (Positive F1-5) from the initial label generation phase of Chain-of-Thought.

Overall, these results indicate GPT-4V's limited ability in identifying medical conditions from chest X-ray images, regardless of whether labels are derived from CoT 1st step or direct prompting.

Testing whether GPT-4V generates labels based on given chest X-rays. Considering the failure of GPT-4V to accurately label medical conditions, we would like to investigate to what extent can GPT-4V predict meaningful labels given a specific chest X-ray image. To test this, we group chest X-rays by their groundtruth conditions and then analyze the generated label distribution for each group. If the label distributions are similar across different condition groups, it would suggest that GPT-4V is not meaningfully identifying labels from the chest X-rays but rather assigning labels randomly without proper image interpretation. For example, if the model's generated label probabilities are roughly the same regardless of whether the groundtruth condition of the given image is Edema or Cardiomegaly, it indicates a limited capability in medical image reasoning.

Formally, let X_{ij} be a binary random variable that takes the value 1 if GPT-4V labels the j-th condition as positive for the chest X-ray image associated with the i-th study, and 0 otherwise, where $i = 1, 2, \ldots, 300$ and $j = 1, 2, \ldots, 13$. We exclude the "No Findings" condition from this study. We define $Y_j = \sum_{i=1}^{300} X_{ij}$ as the sum of positive mentions for the j-th condition across all 300 studies, and $\mathbf{Y} = [Y_1, \ldots, Y_{13}]$ as the count vector. Next, we categorize the study pool into 13 condition groups, where group k consists all studies that are ground truth positive for the k-th condition based on the associated radiology report. Note that there might be overlaps between these groups, as a single study can be positive for multiple conditions. For each group k, GPT-4V's labeling process given the chest X-ray image from i-th study can be modeled as:

Statistics	Overall		Top 5 Conditions	
	Groundtruth	GPT-4o	Groundtruth	GPT-4o
χ^2 statistic	1770.38	66.05	243.51	5.30
p-value	p < 1e-4	1.00	p < 1e-4	0.994
df.	144	144	16	16

Table 4: χ^2-test for homogeneity of label distribution across different condition groups. When p-value is smaller than 0.0001, at 0.01% significance level, we can reject the null hypothesis that different groups follow the same label distribution.

$$
\begin{cases}
X_{ij}^{(k)} \sim \text{Bernoulli}(P_j^{(k)}) \\
\qquad \text{for } i \in \text{group } k \text{ and } j = 1, \ldots, 13 \\
\mathbf{Y}_k \sim \text{Multinomial}(n_k; \mathbf{P}_k) \\
\qquad \text{with } \mathbf{P}_k = [P_1^{(k)}, \ldots, P_{13}^{(k)}]
\end{cases}
$$
(1)

where n_k is the number of studies in group k, and $P_j^{(k)}$ is the probability that GPT-4V labels the j-th condition as positive for the chest X-ray images associated with the studies in group k.

We first use a χ^2-**test** to test if GPT-4V follows the same label distribution across different groups, i.e., testing the null hypothesis (H_0) that $\mathbf{P}_k = \mathbf{P}_{k'}$ for any groups k and k'. Additionally, we use **bootstrap confidence interval** (Davison and Hinkley, 1997) to test if GPT-4V labels one certain condition independently of the groundtruth condition group. Specifically, we test the null hypothesis (H_0) that $P_j^{(k)} = P_j$ for any condition j and group k. More test details and robustness check can be found in Appendix C.1.

Table 4 presents χ^2-test results for the homogeneity of label distribution across different groups. For both the overall and top 5 conditions[5], at 0.01% significance level, we can both reject the null hypothesis for groundtruth reports that different groups follow the same label distribution, but not for GPT-4V's generated reports.

Figure 3 illustrates the 95% bootstrap confidence intervals for top 5 conditions[6]. If zero falls within the interval, we cannot reject the null hypothesis that GPT-4V labels the j-th condition independently of the condition group at 95% confidence level. The figure shows that, in 7 out of 12 cases

---

[5]Due to the sparsity of the original study pool, we report results for two different tables: (1) A modified table with zero elements replaced by 0.001; (2) A reduced table with only five most frequent medical conditions in the subsample.

[6]Due to the sparsity of the original study pool, we limit our analysis to the five most frequent medical conditions in our subsample.
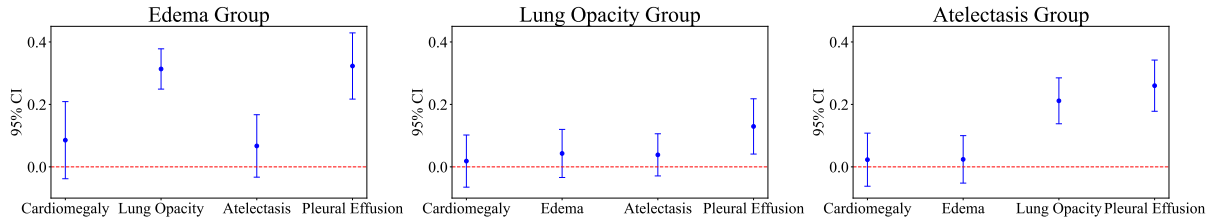
Figure 2: 95% Bootstrap confidence interval of example 3 conditions for MIMIC-CXR. When zero falls into the interval, at 95% confidence level, we cannot reject the null hypothesis that GPT-4V labels j-th condition independent of which condition group this study belongs to.

Experiment	Lexical metrics				Clinic Efficacy Metrics					
	BLEU-1	BLEU-4	ROUGE	METEOR	Pos F1	Pos F1@5	Rad. F1	Neg F1	Neg F1@5	Hall.↓
GPT-4o	0.159	0.006	0.142	0.185	0.123	0.152	0.077	0.038	0.081	0.587
GPT-4o (gt)	0.175	0.009	0.187	0.183	0.879	0.972	0.105	0.639	0.956	**0.427**
GPT-4-vision-preview (gt)	0.176	0.007	0.185	0.179	0.885	**0.977**	0.103	0.584	**0.958**	0.431
Finetuned Llama-2 (gt)	**0.301**	**0.094**	**0.330**	**0.348**	**0.923**	0.957	**0.286**	**0.703**	0.941	0.710

Table 5: Performance in report generation with groundtruth conditions. Although GPT-4V's performance improves significantly, it still underperforms finetuned Llama-2, especially in matching the writing style of groundtruth reports.

(58.3%), we cannot reject the null hypothesis.

In summary, the results show that GPT-4V labels conditions independently of the groundtruth condition, and there is no significant difference in label distributions across groups in GPT-4V's generated reports, unlike the groundtruth reports.

4.3 Experiment 3: Given groundtruth conditions, can GPT-4V generate reports?

Given that GPT-4V cannot perform image reasoning, we investigate whether GPT-4V can generate high-quality radiology reports given groundtruth medical conditions. We conduct an experiment on report synthesis (Prompt 3.1) and use a finetuned Llama-2 model as a baseline for comparison.

Table 5 shows that while using groundtruth conditions significantly enhances GPT-4V's clinical accuracy, it still does not perform as well as the finetuned Llama-2, particularly in matching the content of groundtruth reports. Progress in clinical accuracy is evidenced by large improvements in F1 scores compared to basic generation (Prompt 1.1). However, there are only minor changes in lexical metrics and RadGraph F1, which focus on entity relation matching in groundtruth reports, along with consistently large gaps with finetuned Llama-2, suggest that groundtruth conditions are insufficient to align GPT-4V's writing closely with that of groundtruth reports. The higher scores of the finetuned Llama-2 in lexical metrics also indicate that finetuning open models is an effective way to leverage existing datasets.

Human Evaluation. To further evaluate the quality of GPT-4V-generated reports beyond automatic metrics, we collaborate with two experts: one board-certified and one board-eligible radiologist, to conduct a human evaluation. From our testing set of 300 studies, we randomly select 50 cases for blind human evaluation. Each radiologist is provided with anonymized chest X-ray images and randomly ordered IMPRESSION sections from groundtruth reports, as well as reports generated by Llama-2 and GPT-4V. Both Llama-2 and GPT-4V are prompted with groundtruth medical conditions. The evaluation involves a detailed review of three reports per study case, assessing each report's clinical usability with a binary label as the first step. Then, the radiologist rates each report on two dimensions: clinical efficacy (diagnostic accuracy and completeness) and lexical performance (clarity/readability). Reports are rated on a Likert scale, where a score of 5 denotes superior performance and a score of 1 denotes poor performance. We compute and report the average scores for each metric across different report types.

Table 6 shows that, from the perspective of radiologists, GPT-4V still underperforms the finetuned Llama-2. Groundtruth reports are indeed of high quality, rated as clinically usable in 50 out of 50 cases. However, a significant usability gap is observed between Llama-2 and GPT-4V, with Llama-2 being deemed clinically usable in 46 out of 50 cases, compared to 36 out of 50 for GPT-4V. Furthermore, Llama-2 consistently outperforms GPT-

	Binary	Likert Scale (1-5)		
	Clinically Usable	**Diagnostic Accuracy**	**Completeness**	**Clarity/Readability**
Groundtruth	50/50 (100%)	**4.86**	**4.87**	4.92
Finetuned Llama-2	46/50 (92%)	4.16	4.42	**4.94**
GPT-4-vision-preview	36/50 (72%)	3.63	3.49	3.80

All metrics are evaluated on the impression section and are averaged based on results from two experts.

Table 6: Human evaluation of radiology report quality. From the perspective of radiologists, GPT-4V underperforms relative to the finetuned Llama-2, particularly in fine-grained likert scale metrics of diagnostic accuracy, completeness, and clartiy/readability.

Groundtruth labels	Model	Report	Usable	Acc.	Comp.	Clarity
Positive: Enlarged Cardio-mediastinum, Lung Opacity, Atelectasis Negative: Pneumonia	Groundtruth	In comparison with study of ___, there is little change in the cardiomediastinal silhouette and pacer leads. Continued elevation of the right hemidiaphragmatic contour. Opacification medially above the elevated hemidiaphragm most likely represents atelectatic changes. No definite acute focal pneumonia.	✓	5	5	4
	Finetuned Llama-2	1. No evidence of pneumonia. 2. Stable postoperative appearance of the chest. 3. Increased retrocardiac opacity likely reflects atelectasis.	✓	5	5	5
	GPT-4-vision-preview	The chest radiograph demonstrates an enlarged cardiomediastinum, lung opacity which may be due to various etiologies, and atelectasis. There is no clear evidence of pneumonia on the radiograph.	✓	3	4	3

Table 7: Comparison of example reports from human annotation.

4V across all other Likert scale metrics, especially in completeness and clarity/readability.

Table 7 presents three example reports. While groundtruth reports offer detailed clinical insights and varied descriptors, GPT-4V tends to provide vague statements, only stating "lung opacity which may be due to various etiologies" without specifying its location, severity, or offering a differential diagnosis. Llama-2 performs slightly better by offering some specific diagnoses, yet still lacks detailed descriptions.

In summary, human annotation corroborates with our findings from Experiment 3. Given groundtruth conditions, GPT-4V generated reports still lack comprehensive coverage of all relevant clinical findings and do not effectively summarize and organize medical conditions, compared with human-written reports.

5 Conclusions

We perform the first systematic and in-depth evaluation of the GPT-4V series models in radiology report generation using three chest X-ray benchmarks. We find that GPT-4V cannot generate radiology reports, even with different prompting strategies. Open-sourced models like Llama-3.2 vision perform similarly poorly compared to GPT-4V. Both closed-source and open-source models exhibit a significant gap when compared to specialized SOTA radiology report generation models. To understand the low performance, we decompose the task into image reasoning and report synthesis. The results demonstrate that GPT-4V struggles significantly with interpreting chest X-rays meaningfully, which directly impacts its ability to generate reports. Furthermore, even when we bypass this problem by providing groundtruth conditions, GPT-4V still underperforms a finetuned Llama-2 baseline and consistently fails to replicate the writing style of groundtruth reports or meet the preferences of radiologists. Overall, our study highlights substantial concerns regarding the feasibility of integrating GPT-4V into real radiology workflows.

6 Limitations

In this paper, we utilize the GPT-4 model series and Llama-3.2 to conduct a systematic evaluation of their capabilities in generating radiology

reports. Comparisons with other general-domain multimodal LMMs, including Google's Gemini, are reserved for future research.

Additionally, we use four common prompting strategies in our study and encourage future research to explore additional techniques, such as Self-Critique (Shinn et al., 2023), to verify the robustness of our findings. Due to resource constraints, we randomly select a subset of data for overall evaluation and use 50 samples for a human study. Besides, the human study is limited to two radiologists' subjective assessment, potentially influenced by their personal style and preferences. While our human evaluation could be improved by recruiting more radiologists, we believe that GPT-4's poor performance may not justify a significantly larger human evaluation. That said, our results suggest that finetuned open models may hold the potential of fitting into the current radiologist workflow if we can leverage medical image reasoning abilities of other models.

Despite these limitations, we believe the findings from this paper are well-supported by our comprehensive and detailed evaluation framework. Results from our work raise serious concerns about how to safely integrate general-domain LMMs into real-world radiology workflows. It is worth noting that OpenAI itself restricts the medical use of GPT-4. Experiments using GPT-4o and Llama-3.2 are conducted successfully without any model rejections. However, GPT-4-vision-preview, particularly when using few-shot prompt, will sometimes return "I'm sorry, but I cannot provide a diagnostic report or interpretation for medical images. If you have any medical concerns, please consult a qualified healthcare professional who can provide a proper examination and diagnosis.", while we still get majority of responses from the model, full details can be found in Appendix Table 8.

Acknowledgments

References

Satanjeev Banerjee and Alon Lavie. 2005. Meteor: An automatic metric for mt evaluation with improved correlation with human judgments. In *Proceedings of the acl workshop on intrinsic and extrinsic evaluation measures for machine translation and/or summarization*, pages 65–72.

Rajesh Bhayana, Robert R Bleakney, and Satheesh Krishna. 2023. Gpt-4 in radiology: improvements in advanced reasoning. *Radiology*, 307(5):e230987.

Dana Brin, Vera Sorin, Yiftach Barash, Eli Konen, Benjamin S. Glicksberg, Girish Nadkarni, and Eyal Klang. 2023. Assessing gpt-4 multimodal performance in radiological image analysis. *medRxiv*.

Sébastien Bubeck, Varun Chandrasekaran, Ronen Eldan, Johannes Gehrke, Eric Horvitz, Ece Kamar, Peter Lee, Yin Tat Lee, Yuanzhi Li, Scott Lundberg, et al. 2023. Sparks of artificial general intelligence: Early experiments with gpt-4. *arXiv preprint arXiv:2303.12712*.

Pierre Chambon, Jean-Benoit Delbrouck, Thomas Sounack, Shih-Cheng Huang, Zhihong Chen, Maya Varma, Steven QH Truong, Chu The Chuong, and Curtis P. Langlotz. 2024. Chexpert plus: Augmenting a large chest x-ray dataset with text radiology reports, patient demographics and additional image formats. *Preprint*, arXiv:2405.19538.

Juan Manuel Zambrano Chaves, Shih-Cheng Huang, Yanbo Xu, Hanwen Xu, Naoto Usuyama, Sheng Zhang, Fei Wang, Yujia Xie, Mahmoud Khademi, Ziyi Yang, et al. 2024. Towards a clinically accessible radiology foundation model: open-access and lightweight, with automated evaluation. *Preprint*, arXiv:2403.08002.

Anthony Christopher Davison and David Victor Hinkley. 1997. *Bootstrap methods and their application*. 1. Cambridge university press.

Dina Demner-Fushman, Marc D Kohli, Marc B Rosenman, Sonya E Shooshan, Laritza Rodriguez, Sameer Antani, George R Thoma, and Clement J McDonald. 2016. Preparing a collection of radiology examinations for distribution and retrieval. *Journal of the American Medical Informatics Association*, 23(2):304–310.

Roman Johannes Gertz, Thomas Dratsch, Alexander Christian Bunck, Simon Lennartz, Andra-Iza Iuga, Martin Gunnar Hellmich, Thorsten Persigehl, Lenhard Pennig, Carsten Herbert Gietzen, Philipp Fervers, et al. 2024. Potential of gpt-4 for detecting errors in radiology reports: Implications for reporting accuracy. *Radiology*, 311(1):e232714.

Amir M Hasani, Shiva Singh, Aryan Zahergivar, Beth Ryan, Daniel Nethala, Gabriela Bravomontenegro, Neil Mendhiratta, Mark Ball, Faraz Farhadi, and Ashkan Malayeri. 2023. Evaluating the performance of generative pre-trained transformer-4 (gpt-4) in

standardizing radiology reports. *European Radiology*, pages 1–9.

Stephanie L Hyland, Shruthi Bannur, Kenza Bouzid, Daniel C Castro, Mercy Ranjit, Anton Schwaighofer, Fernando Pérez-García, Valentina Salvatelli, Shaury Srivastav, Anja Thieme, et al. 2023. Maira-1: A specialised large multimodal model for radiology report generation. *arXiv preprint arXiv:2311.13668*.

Jeremy Irvin, Pranav Rajpurkar, Michael Ko, Yifan Yu, Silviana Ciurea-Ilcus, Chris Chute, Henrik Marklund, Behzad Haghgoo, Robyn Ball, Katie Shpanskaya, et al. 2019. Chexpert: A large chest radiograph dataset with uncertainty labels and expert comparison. In *Proceedings of the AAAI conference on artificial intelligence*, volume 33, pages 590–597.

Saahil Jain, Ashwin Agrawal, Adriel Saporta, Steven QH Truong, Du Nguyen Duong, Tan Bui, Pierre Chambon, Yuhao Zhang, Matthew P Lungren, Andrew Y Ng, et al. 2021. Radgraph: Extracting clinical entities and relations from radiology reports. *arXiv preprint arXiv:2106.14463*.

A Johnson, T Pollard, R Mark, S Berkowitz, and Steven Horng. 2019. Mimic-cxr database (version 2.0. 0). *physionet*, 2:5.

Yingshu Li, Yunyi Liu, Zhanyu Wang, Xinyu Liang, Lingqiao Liu, Lei Wang, Leyang Cui, Zhaopeng Tu, Longyue Wang, and Luping Zhou. 2023. A comprehensive study of gpt-4v's multimodal capabilities in medical imaging. *medRxiv*, pages 2023–11.

Chin-Yew Lin. 2004. Rouge: A package for automatic evaluation of summaries. In *Text summarization branches out*, pages 74–81.

Chang Liu, Yuanhe Tian, Weidong Chen, Yan Song, and Yongdong Zhang. 2024a. Bootstrapping large language models for radiology report generation. In *Proceedings of the AAAI Conference on Artificial Intelligence*, volume 38, pages 18635–18643.

Fenglin Liu, Hongjian Zhou, Yining Hua, Omid Rohanian, Lei Clifton, and David Clifton. 2024b. Large language models in healthcare: A comprehensive benchmark. *medRxiv*, pages 2024–04.

Qianchu Liu, Stephanie Hyland, Shruthi Bannur, Kenza Bouzid, Daniel C Castro, Maria Teodora Wetscherek, Robert Tinn, Harshita Sharma, Fernando Pérez-García, Anton Schwaighofer, et al. 2023a. Exploring the boundaries of gpt-4 in radiology. *arXiv preprint arXiv:2310.14573*.

Zhengliang Liu, Hanqi Jiang, Tianyang Zhong, Zihao Wu, Chong Ma, Yiwei Li, Xiaowei Yu, Yutong Zhang, Yi Pan, Peng Shu, et al. 2023b. Holistic evaluation of gpt-4v for biomedical imaging. *arXiv preprint arXiv:2312.05256*.

Dang Nguyen, Chacha Chen, He He, and Chenhao Tan. 2023. Pragmatic radiology report generation. In *Machine Learning for Health (ML4H)*, pages 385–402. PMLR.

Harsha Nori, Nicholas King, Scott Mayer McKinney, Dean Carignan, and Eric Horvitz. 2023. Capabilities of gpt-4 on medical challenge problems. *arXiv preprint arXiv:2303.13375*.

Kishore Papineni, Salim Roukos, Todd Ward, and Wei-Jing Zhu. 2002. Bleu: a method for automatic evaluation of machine translation. In *Proceedings of the 40th annual meeting of the Association for Computational Linguistics*, pages 311–318.

Noah Shinn, Beck Labash, and Ashwin Gopinath. 2023. Reflexion: an autonomous agent with dynamic memory and self-reflection. *arXiv preprint arXiv:2303.11366*.

Akshay Smit, Saahil Jain, Pranav Rajpurkar, Anuj Pareek, Andrew Y Ng, and Matthew P Lungren. 2020. Chexbert: combining automatic labelers and expert annotations for accurate radiology report labeling using bert. *arXiv preprint arXiv:2004.09167*.

Zhaoyi Sun, Hanley Ong, Patrick Kennedy, Liyan Tang, Shirley Chen, Jonathan Elias, Eugene Lucas, George Shih, and Yifan Peng. 2023. Evaluating gpt-4 on impressions generation in radiology reports. *Radiology*, 307(5):e231259.

Rohan Taori, Ishaan Gulrajani, Tianyi Zhang, Yann Dubois, Xuechen Li, Carlos Guestrin, Percy Liang, and Tatsunori B Hashimoto. 2023. Alpaca: A strong, replicable instruction-following model. *Stanford Center for Research on Foundation Models. https://crfm. stanford. edu/2023/03/13/alpaca. html*, 3(6):7.

Tao Tu, Shekoofeh Azizi, Danny Driess, Mike Schaekermann, Mohamed Amin, Pi-Chuan Chang, Andrew Carroll, Charles Lau, Ryutaro Tanno, Ira Ktena, et al. 2024. Towards generalist biomedical ai. *NEJM AI*, 1(3):AIoa2300138.

Jason Wei, Xuezhi Wang, Dale Schuurmans, Maarten Bosma, Fei Xia, Ed Chi, Quoc V Le, Denny Zhou, et al. 2022. Chain-of-thought prompting elicits reasoning in large language models. *Advances in neural information processing systems*, 35:24824–24837.

Chaoyi Wu, Jiayu Lei, Qiaoyu Zheng, Weike Zhao, Weixiong Lin, Xiaoman Zhang, Xiao Zhou, Ziheng Zhao, Ya Zhang, Yanfeng Wang, et al. 2023. Can gpt-4v (ision) serve medical applications? case studies on gpt-4v for multimodal medical diagnosis. *arXiv preprint arXiv:2310.09909*.

Zhiling Yan, Kai Zhang, Rong Zhou, Lifang He, Xiang Li, and Lichao Sun. 2023. Multimodal chatgpt for medical applications: an experimental study of gpt-4v. *arXiv preprint arXiv:2310.19061*.

Zhengyuan Yang, Linjie Li, Kevin Lin, Jianfeng Wang, Chung-Ching Lin, Zicheng Liu, and Lijuan Wang. 2023. The dawn of lmms: Preliminary explorations with gpt-4v (ision). *arXiv preprint arXiv:2309.17421*, 9(1):1.

A Model Impementation Details

OpenAI API: We evaluate three datasets using Microsoft's Azure OpenAI service with GPT-4-vision-preview (11/15/2023) and GPT-4o.

Finetuning Llama-2: In the case of the MIMIC dataset, we selectively sample 10% of the official training data, carefully ensuring there is no overlap with the 300-sample test set. For the IU X-ray dataset, we utilize the entire training set, which comprises 3,655 studies, and confirm that these too do not overlap with the test set. The fine-tuning process largely adheres to the default hyperparameters established by Stanford Alpaca (Taori et al., 2023). Our hardware includes four A100 GPUs, each equipped with 80GiB of memory, and operates on CUDA version 12.4.

Llama-3.2-90B-Vision-Instruct: Llama-3.2-90B-Vision is the newest flagship open-source multimodal LLM. We choose it to provide a baseline reference. We access the model weights through huggingface and Meta. Our hardware for inference includes four A100 GPUs, each equipped with 80GiB of memory, and operates on CUDA version 12.4.

Code Availability: The source code for our project is publicly accessible on GitHub, enabling users and fellow researchers to review, utilize, or extend our implementations. You can find our repository at `https://github.com/ChicagoHAI/cxr-eval-gpt-4v.git`.

B Data

Data licenses: MIMIC-CXR license can be found at `https://physionet.org/content/mimic-cxr/view-license/2.0.0/`. IU X-RAY images are distributed under the terms of the Creative Commons Attribution-NonCommercial-NoDerivatives 4.0 International License (`http://creativecommons.org/licenses/by-nc-nd/4.0/`).

For MIMIC-CXR, we accessed the data by following the required steps on `https://physionet.org/content/mimic-cxr/2.0.0/`. We first registered and applied to be a credentialed user, and then completed the required training of CITI Data or Specimens Only Research. We also signed the data use agreement for the project before we get access to the dataset. We downloaded IU X-RAY dataset from `https://openi.nlm.nih.gov/faq`.

Chexpert Plus dataset is available to download online and the license can be found at `https://stanfordaimi.azurewebsites.net/datasets/5158c524-d3ab-4e02-96e9-6ee9efc110a1`.

Preprocessing: To prepare the data for the OpenAI API, we first convert the DICOM images to JPEG format, which is required for compatibility with GPT-4V. Then we use base64 encoding to transform the binary image data into its corresponding UTF-8 string.

Ethical consideration of data: There is no substantial concerns around the data, since dataset are de-identified and do not contain harmful or offensive contents.

C Experiment Results

C.1 Hypothesis Test

Bootstrap Confidence Interval We use **bootstrap confidence interval** (Davison and Hinkley, 1997) to test if GPT-4V labels one certain condition independently of the groundtruth condition group. For this test, for each condition i and group j, we define test statistic θ_{ij} as $P_i^{(j)} - P_i$ and null hypothesis H_0 as $\theta_{ij} = 0$. We construct a 95% confidence interval as $[\hat{\theta}_{ij,\,0.025}^{(B)}, \hat{\theta}_{ij,\,0.975}^{(B)}]$ with 1000 bootstrap samples for each θ_{ij}. Considering the sparsity of original study pool, we limit our choice of condition i and group j in six most frequent conditions in our subsample.

χ^2 Test Specifically, we use a χ^2-**test** to test if GPT-4V follows the same label distribution across different groups, i.e., testing the null hypothesis (H_0) that $\mathbf{P}_k = \mathbf{P}_{k'}$ for any groups k and k'. For the overall pool, we can construct a 13×13 contingency table with each entry equal to $Y_i^{(j)}$ and then calculate expected count $E_i^{(j)}$ for each entry. Finally, report $\chi^2 = \sum_i \sum_j \frac{(Y_i^{(j)} - E_i^{(j)})^2}{E_i^{(j)}}$. Considering the sparsity of original study pool, we report results of two different tables: (1) A modified table that replaces zero elements with 0.001; (2) A reduced table with only six most frequent conditions in subsample.

Pearson Correlation Coefficient We approximate $P_j^{(k)}$ using $\Pr(X_{ij}^{(k)} = 1)$ to obtain an estimator $\widehat{\mathbf{P}}_k$ of $\mathbf{P}_k$ for each group k. Furthermore, we illustrate the correlation $\text{Corr}(\widehat{\mathbf{P}}_m, \widehat{\mathbf{P}}_n)$ for all groups m and n in Figure 5 and Figure 6. It is noted

that the condition "Pleural Other" doesn't seem to be highly correlated with other groups. However, considering that "Pleural Other" only has one positive mention in groundtruth conditions and this can be treated as an outlier.

Robustness Check We look into overlap issue between any two groups to further verify our results' robustness. We find out that it does not compromise the assumptions of the multinomial distribution or the robustness of Bootstrap CI results, but it could potentially inflate the Chi-square statistic, leading to incorrect conclusion about "no significance". To affirm the integrity of our Chi-square test results, we highlight two points: first, comparison with groundtruth studies in Table 4 shows a distinct difference in p-values (small for groundtruth and large for generated studies), suggesting minimal impact of overlap on our conclusion that "GPT-4V generates reports following the same label distribution." Additionally, we also check the overlapped samples between groups and find them to be relatively small to original group sizes, with an average ratio of 13.1%, as detailed in Figure 7.

C.2 GPT-4o Evaluation

Overall performance of direct report generation across three datasets is shown in Table 10, Table 11 and Table 12. Complete image reasoning results can be seen in Table 16. Complete Chi square test can be seen in Table 17.

C.3 GPT-4-vision-preview Evaluation

Medical Restriction in Usage of GPT-4V API Since OpenAI itself will restrict the medical use of GPT-4V, the actual sample size of our expriments will be smaller than 300. Details can be checked in Table 8.

Misspecification of Negative Mentions in GPT-4V Besides, it is noted that the "negative" category in 2-class labeling actually includes negative, uncertain, and unmentioned mentions. However, GPT-4V shows very similar Negative F1 scores across different labeling types. This suggests that GPT-4V often incorrectly labels uncertain and unmentioned conditions as negative, contributing to its poor performance in accurately identifying negative mentions. More evidence on label distribution is available in Table 9.

Overall Results of GPT-4V Table 13 and Table 14 show all results on both findings section and impression section. Complete image reasoning results can be seen in Table 15. Complete Chi square test can be seen in Table 18. Table 19 show the generated results with groundtruth conditions.

C.4 Llama-3.2-90B-Vision Evaluation

Overall performance of direct report generation across three datasets is shown in Table 20, Table 21 and Table 22. It is noted that low hallucination of Llama-generated reports is probably due to its straightforward and assertive writing style, exemplified by sentences such as "The heart is enlarged," "There is a left pleural effusion," and "There is a right lung opacity."

C.5 Examples of Generated Reports

The generated examples by different prompting strategies are shown in table 23.

D Human Reader Study

Instructions for human study are shown in Figure 8.

Experiment	IU X-RAY			MIMIC-CXR		
	IMPRESSION	FINDINGS	Labels	IMPRESSION	FINDINGS	Labels
1.1	298/300	259/260	-	300/300	183/183	-
1.2	295/300	259/260	-	300/300	183/183	-
1.3	278/300	241/260	-	300/300	183/183	-
1.4	258/300	223/260	-	300/300	183/183	-
1.5	118/300	101/260	-	83/300	61/183	-
2.1	-	-	237/300	-	-	300/300
3.1	293/300	253/260	-	297/300	182/183	-

Table 8: Summary of actual sample size across different experiments.

Condition	GT					2.1			2.2				
	Pos	Neg	Unc	Unmnt	Pr(Pos)	Pos	Other	Pr(Pos)	Pos	Neg	Unc	Unmnt	Pr(Pos)
Edema	35	42	15	208	0.117	46	254	0.153	76	174	0	50	0.253
Consolidation	10	17	5	268	0.033	18	282	0.060	30	234	0	36	0.100
Pneumonia	7	37	24	232	0.023	6	294	0.020	14	242	0	44	0.047
Pneumothorax	7	45	3	245	0.023	6	294	0.020	5	272	0	23	0.017
Pleural Effusion	65	30	3	202	0.217	190	110	0.633	212	77	0	11	0.707

Table 9: Label distribution of top 5 conditions (MIMIC-CXR).

Table 10: Direct report generation performance comparison for IU X-ray findings and impressions (GPT-4o).

Experiment	Lexical metrics				Clinical Efficacy Metrics					
	BLEU-1	BLEU-4	ROUGE-L	METEOR	Pos F1	Pos F1@5	RadGraph	Neg F1	Neg F1@5	Hall.↓
IU X-RAY (FINDINGS)										
1.1	0.316	0.045	0.238	0.311	0.059	0.045	0.203	0.272	0.397	0.354
1.2	0.330	0.049	0.242	0.323	0.077	0.098	0.214	0.285	0.419	0.269
1.3	0.238	0.030	0.207	0.283	0.081	0.146	0.174	0.298	0.458	0.169
1.4	0.239	0.024	0.194	0.231	0.077	0.161	0.144	0.285	0.440	0.138
1.5	0.279	0.044	0.243	0.250	0.037	0.031	0.187	0.240	0.379	0.097
IU X-RAY (IMPRESSION)										
1.1	0.212	0.012	0.194	0.269	0.087	0.105	0.104	0.000	0.000	0.303
1.2	0.248	0.014	0.251	0.341	0.173	0.135	0.153	0.071	0.051	0.307
1.3	0.209	0.012	0.205	0.281	0.111	0.206	0.106	0.000	0.000	0.177
1.4	0.181	0.007	0.143	0.177	0.115	0.255	0.060	0.000	0.000	0.197
1.5	0.138	0.001	0.077	0.124	0.067	0.107	0.034	0.010	0.025	0.211

Table 11: Performance comparison for MIMIC-CXR findings and impressions (GPT-4o).

Experiment	Lexical metrics				Clinical Efficacy Metrics					
	BLEU-1	BLEU-4	ROUGE-L	METEOR	Pos F1	Pos F1@5	RadGraph	Neg F1	Neg F1@5	Hall.↓
MIMIC-CXR (FINDINGS)										
1.1	0.331	0.031	0.225	0.282	0.134	0.153	0.163	0.244	0.418	0.421
1.2	0.333	0.044	0.234	0.290	0.273	0.255	0.182	0.259	0.431	0.383
1.3	0.276	0.028	0.203	0.264	0.155	0.230	0.154	0.290	0.503	0.298
1.4	0.242	0.017	0.186	0.201	0.172	0.272	0.119	0.249	0.443	0.180
1.5	0.337	0.055	0.257	0.301	0.170	0.203	0.188	0.279	0.481	0.934
MIMIC-CXR (IMPRESSION)										
1.1	0.159	0.006	0.142	0.185	0.123	0.152	0.077	0.038	0.081	0.587
1.2	0.203	0.014	0.195	0.238	0.277	0.258	0.124	0.048	0.126	0.547
1.3	0.168	0.009	0.162	0.200	0.156	0.243	0.095	0.042	0.101	0.359
1.4	0.120	0.004	0.112	0.130	0.177	0.288	0.055	0.008	0.020	0.397
1.5	0.155	0.007	0.153	0.186	0.144	0.232	0.073	0.035	0.091	0.477

Table 12: Performance comparison for ChexPert Plus findings and impressions (GPT-4o).

Experiment	Lexical metrics				Clinical Efficacy Metrics					
	BLEU-1	BLEU-4	ROUGE-L	METEOR	Pos F1	Pos F1@5	RadGraph	Neg F1	Neg F1@5	Hall.↓
CHEXPERT PLUS (FINDINGS)										
1.1	0.237	0.015	0.176	0.191	0.228	0.191	0.112	0.118	0.174	0.516
1.3	0.191	0.007	0.159	0.172	0.210	0.325	0.101	0.158	0.253	0.371
1.4	0.166	0.011	0.155	0.139	0.234	0.339	0.077	0.160	0.262	0.339
1.5	0.171	0.007	0.158	0.149	0.188	0.224	0.094	0.104	0.135	0.411
3.1	0.085	0.003	0.150	0.108	0.483	0.724	0.080	0.148	0.250	0.226
CHEXPERT PLUS (IMPRESSION)										
1.1	0.105	0.001	0.106	0.090	0.163	0.198	0.008	0.013	0.035	0.680
1.3	0.109	0.002	0.105	0.095	0.172	0.261	0.008	0.042	0.085	0.377
1.4	0.066	0.000	0.093	0.069	0.192	0.242	0.012	0.000	0.000	0.400
1.5	0.084	0.002	0.131	0.088	0.134	0.161	0.029	0.043	0.111	0.370
3.1	0.106	0.003	0.164	0.116	0.854	0.947	0.022	0.662	0.924	0.480

Experiment	Lexical metrics				Clinic Efficacy Metrics					
	BLEU-1	BLEU-4	ROUGE	METEOR	Pos F1	Pos F1@5	Rad. F1	Neg F1	Neg F1@5	Hall.↓
MIMIC-CXR (FINDINGS)										
1.1	0.299	0.035	0.214	0.279	0.117	0.124	0.135	0.241	0.396	0.563
1.2	0.323	0.042	0.227	0.294	0.181	0.194	0.159	0.272	0.464	0.410
1.3	0.265	0.019	0.186	0.262	0.134	0.236	0.109	0.237	0.437	0.607
1.4	0.236	0.008	0.176	0.202	0.151	0.233	0.080	0.151	0.328	0.563
1.5	0.294	0.053	0.223	0.293	0.085	0.036	0.149	0.251	0.462	1.000
MIMIC-CXR (IMPRESSION)										
1.1	0.135	0.018	0.119	0.161	0.118	0.160	0.071	0.004	0.001	0.687
1.2	0.176	0.021	0.163	0.200	0.185	0.200	0.101	0.037	0.096	0.610
1.3	0.141	0.009	0.120	0.174	0.141	0.228	0.068	0.026	0.067	0.593
1.4	0.113	0.002	0.107	0.133	0.150	0.255	0.058	0.023	0.061	0.607
1.5	0.163	0.011	0.160	0.242	0.070	0.072	0.088	0.000	0.000	0.578

Table 13: Direct report generation performance comparison for MIMIC-CXR findings and impressions (GPT-4-vision-preview).

Experiment	Lexical metrics				Clinic Efficacy Metrics					
	BLEU-1	BLEU-4	ROUGE	METEOR	Pos F1	Pos F1@5	Rad. F1	Neg F1	Neg F1@5	Hall.↓
IU X-RAY (FINDINGS)										
1.1	0.278	0.038	0.218	0.326	0.030	0.024	0.178	0.284	0.429	0.494
1.2	0.282	0.042	0.216	0.328	0.023	0.010	0.174	0.308	0.475	0.614
1.3	0.237	0.027	0.189	0.281	0.053	0.052	0.140	0.265	0.429	0.523
1.4	0.233	0.016	0.179	0.235	0.072	0.119	0.105	0.226	0.402	0.619
1.5	0.325	0.037	0.247	0.318	0.061	0.080	0.191	0.290	0.455	0.287
IU X-RAY (IMPRESSION)										
1.1	0.219	0.019	0.232	0.295	0.036	0.041	0.155	0.000	0.000	0.275
1.2	0.209	0.021	0.215	0.295	0.058	0.060	0.169	0.020	0.052	0.410
1.3	0.202	0.013	0.205	0.287	0.041	0.051	0.142	0.041	0.106	0.435
1.4	0.172	0.009	0.155	0.216	0.052	0.100	0.097	0.000	0.000	0.628
1.5	0.247	0.026	0.243	0.279	0.036	0.047	0.138	0.026	0.067	0.263

Table 14: Direct report generation performance comparison for IU X-RAY findings and impressions (GPT-4-vision-preview).

Metric	MIMIC-CXR		IU X-RAY	
	Chain-of-Thought (1st Step)	Image Reasoning	Chain-of-Thought (1st Step)	Image Reasoning
Positive F1	0.166	0.146	0.072	0.049
Positive F1@5	0.261	0.208	0.095	0.056

Table 15: Image reasoning performance of GPT-4-vision-preview on chest X-ray images.

Metric	MIMIC-CXR		CheXpert Plus	
	Chain-of-Thought (1st Step)	Image Reasoning	Chain-of-Thought (1st Step)	Image Reasoning
Positive F1	0.195	0.161	0.221	0.189
Positive F1@5	0.298	0.242	0.257	0.247

Table 16: Image reasoning performance of GPT-4o on chest X-ray images.

	MIMIC				CheXpert Plus			
	Overall (GT)	Overall (Gen)	Top 6 (GT)	Top 6 (Gen)	Overall (GT)	Overall (Gen)	Top 6 (GT)	Top 6 (Gen)
χ^2 statistic	1770.38	66.05	317.86	8.71	1546.86	53.24	309.31	3.88
p-value	p<1e-1	1	p<1e-1	0.9989	p<1e-1	1	p<1e-1	1
df.	144	144	25	25	144	144	25	25

Table 17: χ^2-test for homogeneity of label distribution across different condition groups (GPT-4o).

Statistics	Overall		Top 6 Conditions	
	Groundtruth	GPT-4V	Groundtruth	GPT-4V
χ^2 statistic	1770.38	74.25	317.86	6.11
p-value	p < 1e-4	1.00	p < 1e-4	1.00
df.	144	144	25	25

Table 18: χ^2-test for homogeneity of label distribution across different condition groups (GPT-4-vision-preview).

Experiment	Lexical metrics				Clinic Efficacy Metrics					
	BLEU-1	BLEU-4	ROUGE	METEOR	Pos F1	Pos F1@5	Rad. F1	Neg F1	Neg F1@5	Hall.↓
					MIMIC-CXR					
GPT-4V	0.135	0.018	0.119	0.161	0.118	0.160	0.071	0.004	0.001	0.687
GPT-4V (gt)	0.176	0.007	0.185	0.179	0.885	**0.977**	0.103	0.584	**0.958**	**0.431**
LLaMA-2 (gt)	**0.301**	**0.094**	**0.330**	**0.348**	**0.923**	0.957	**0.286**	**0.703**	0.941	0.710
					IU X-RAY					
GPT-4V	0.219	0.019	0.232	0.295	0.036	0.041	0.155	0.000	0.000	0.275
GPT-4V (gt)	0.216	0.003	0.229	0.207	0.852	0.919	0.089	**0.630**	0.868	0.235
LLaMA-2 (gt)	**0.454**	**0.124**	**0.460**	**0.441**	**0.871**	**0.928**	**0.297**	0.627	**0.963**	**0.110**

All metrics are evaluated on the impression section.

Table 19: Performance in report generation with groundtruth conditions (GPT-4-vision-preiew).

Experiment	Lexical metrics				Clinical Efficacy Metrics					
	BLEU-1	BLEU-4	ROUGE-L	METEOR	Pos F1	Pos F1@5	RadGraph	Neg F1	Neg F1@5	Hall.
				MIMIC-CXR (FINDINGS)						
1.1	0.258	0.026	0.236	0.216	0.159	0.266	0.123	0.200	0.267	0.607
1.2	0.251	0.020	0.249	0.215	0.123	0.217	0.144	0.214	0.305	0.710
1.3	0.110	0.012	0.114	0.122	0.118	0.221	0.073	0.054	0.111	0.262
1.4	0.015	0.000	0.051	0.032	0.172	0.300	0.010	0.024	0.045	0.197
1.5	0.233	0.023	0.233	0.202	0.144	0.249	0.120	0.197	0.270	0.579
				MIMIC-CXR (IMPRESSION)						
1.1	0.089	0.001	0.085	0.094	0.121	0.231	0.036	0.000	0.000	0.161
1.2	0.085	0.000	0.076	0.088	0.132	0.186	0.028	0.000	0.000	0.200
1.3	0.089	0.001	0.089	0.100	0.141	0.215	0.046	0.045	0.117	0.049
1.4	0.095	0.001	0.068	0.081	0.194	0.334	0.022	0.000	0.000	0.990
1.5	0.086	0.000	0.081	0.088	0.111	0.216	0.035	0.000	0.000	0.160

Table 20: Direct report generation performance comparison for MIMIC-CXR findings and impressions (Llama-3.2-90B-Vision-Instruct).

Experiment	Lexical metrics				Clinical Efficacy Metrics					
	BLEU-1	BLEU-4	ROUGE-L	METEOR	Pos F1	Pos F1@5	RadGraph	Neg F1	Neg F1@5	Hall.
				IU X-RAY (FINDINGS)						
1.1	0.248	0.018	0.231	0.231	0.064	0.075	0.146	0.220	0.255	0.404
1.2	0.244	0.019	0.239	0.216	0.021	0.056	0.156	0.221	0.265	0.342
1.3	0.203	0.027	0.190	0.187	0.068	0.082	0.138	0.170	0.308	0.142
1.4	0.015	0.001	0.053	0.037	0.104	0.214	0.008	0.010	0.012	0.677
1.5	0.231	0.018	0.236	0.221	0.061	0.094	0.158	0.227	0.278	0.579
				IU X-RAY (IMPRESSION)						
1.1	0.117	0.000	0.063	0.102	0.054	0.087	0.019	0.000	0.000	0.057
1.2	0.117	0.000	0.058	0.094	0.080	0.197	0.015	0.000	0.000	0.043
1.3	0.096	0.000	0.059	0.104	0.058	0.072	0.023	0.012	0.030	0.011
1.4	0.049	0.000	0.054	0.053	0.082	0.186	0.003	0.015	0.040	0.983
1.5	0.114	0.000	0.065	0.100	0.063	0.102	0.018	0.000	0.000	0.037

Table 21: Direct report generation performance comparison for IU X-RAY findings and impressions (Llama-3.2-90B-Vision-Instruct).

Experiment	Lexical metrics				Clinical Efficacy Metrics					
	BLEU-1	BLEU-4	ROUGE-L	METEOR	Pos F1	Pos F1@5	RadGraph	Neg F1	Neg F1@5	Hall. Prop.
				CHEXPERT PLUS (FINDINGS)						
1.1	0.166	0.006	0.175	0.147	0.214	0.290	0.092	0.096	0.153	0.419
1.3	0.079	0.004	0.100	0.088	0.230	0.266	0.069	0.069	0.180	0.339
1.4	0.022	0.003	0.062	0.029	0.247	0.355	0.006	0.042	0.059	0.097
1.5	0.152	0.005	0.173	0.131	0.261	0.285	0.092	0.109	0.170	0.355
				CHEXPERT PLUS (IMPRESSION)						
1.1	0.073	0.002	0.106	0.072	0.152	0.221	0.013	0.003	0.007	0.173
1.3	0.086	0.002	0.100	0.084	0.174	0.238	0.013	0.031	0.081	0.058
1.4	0.091	0.000	0.087	0.071	0.190	0.281	0.005	0.000	0.000	0.985
1.5	0.067	0.001	0.102	0.069	0.154	0.209	0.012	0.003	0.007	0.157

Table 22: Performance comparison for Chexpert Plus findings and impressions (Llama-3.2-90B-Vision-Instruct).
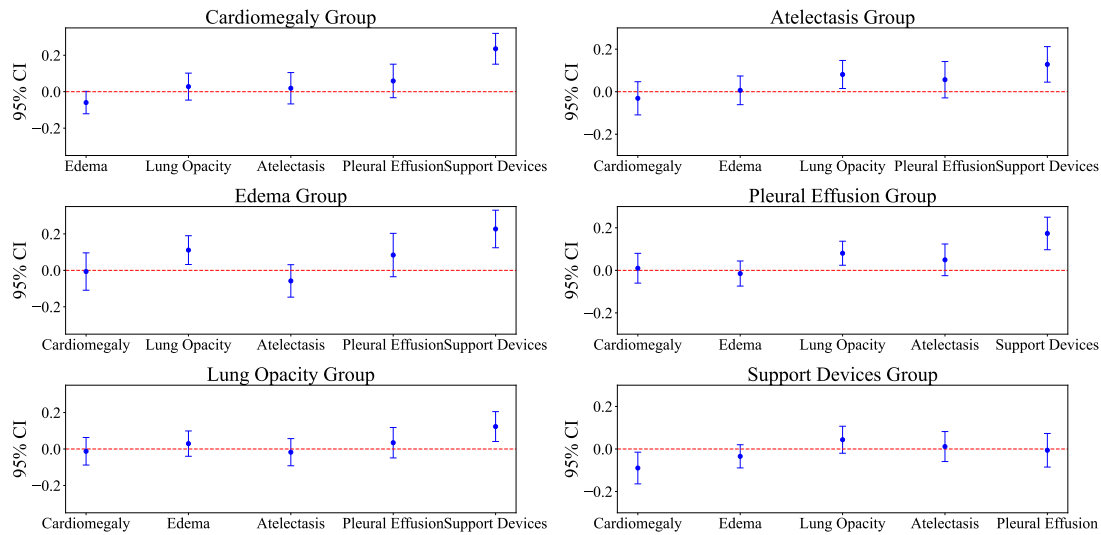
Figure 3: 95% Bootstrap confidence interval of top 6 conditions in our sample for GPT-4-vision-preview.
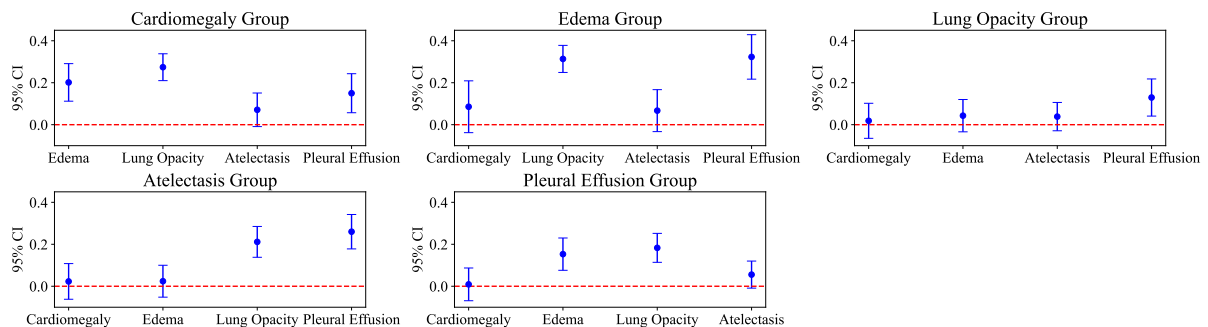
Figure 4: 95% Bootstrap confidence interval of top 5 conditions in our sample for GPT-4o.
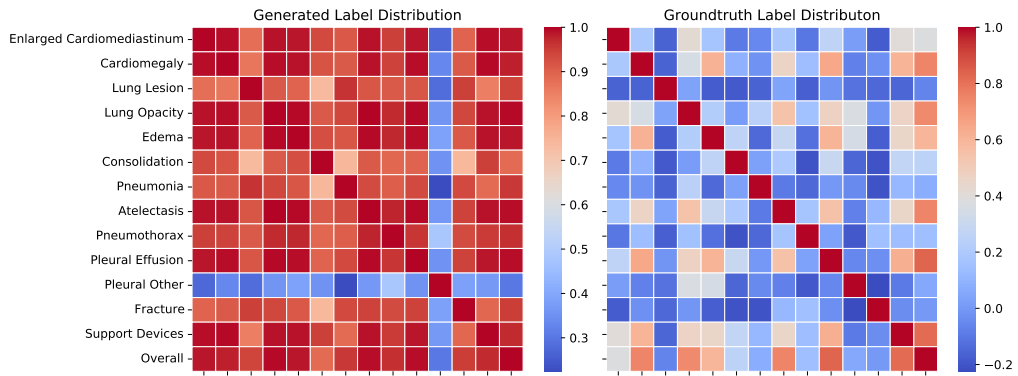
Figure 5: Correlations between distributions of Pr(Pos) for different condition groups (GPT-4-vision-preview).
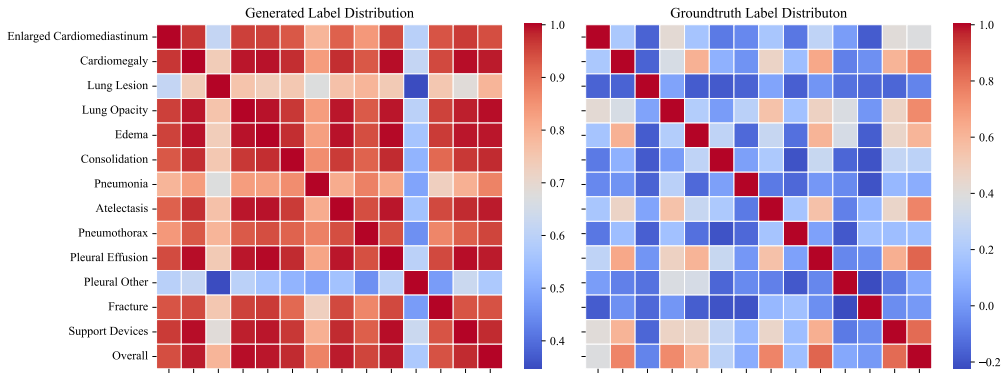

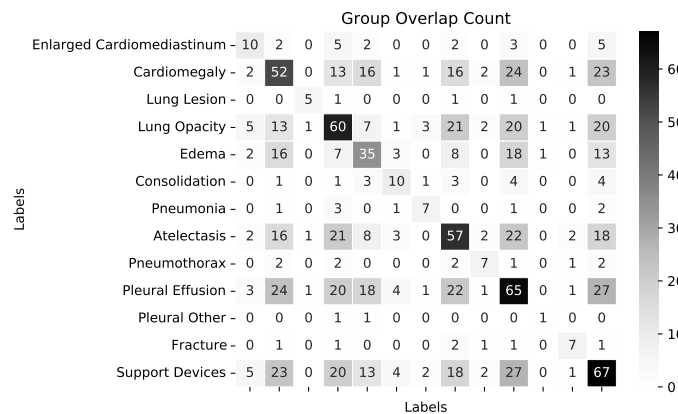Figure 6: Correlations between distributions of Pr(Pos) for different condition groups (GPT-4o).

Figure 7: Overlap count heatmap within groudtruth condition groups. The overlap between any two groups is relatively small compared to the original group sizes, which relate to the counts on the diagonal, ensuring that this overlap does not compromise the robustness of our results.

Experiment	Findings	Impression
GroundTruth	Single AP view of the chest provided. Interval increase in opacification of the right hemithorax with unchanged rightward shift of midline structures. The left lung is clear. Hilar and cardiomediastinal contours are obscured.	Worsening collapse of the right lung from ___ with unchanged rightward shift of mediastinal structures.
Basic	The cardiomediastinal silhouette is severely enlarged. There is opacification of the right hemithorax with loss of visualization of the right heart border; this may be attributable to a large pleural effusion, consolidation, or a combination of both. The left lung field remains clear with normal aeration, without evidence of focal consolidation. The trachea is midline. There is no evidence of pneumothorax on the left. The osseous structures of the visualized portion of the thorax appear intact. Nasogastric tube is in place with its tip projecting over the gastric bubble.	1. Severe cardiomegaly. 2. Opacification of the right hemithorax consistent with a large pleural effusion and/or consolidation. 3. No pneumothorax or acute bony abnormality identified. 4. The presence of a nasogastric tube with an appropriately situated tip. Further investigation with a CT scan may be considered to differentiate between effusion and consolidation and to assess for any additional intrathoracic pathology. Clinical correlation is recommended.
+Indication	The cardiac silhouette appears enlarged. There is an opacity in the right upper lobe consistent with lobar collapse and volume loss as evidenced by crowding of adjacent rib spaces. There are also patchy infiltrates seen in the right lower lobe. The remaining lung fields are clear without evidence of pleural effusion. The bony thorax and soft tissues appear unremarkable.	Right upper lobe and right lower lobe collapse with an enlarged cardiac silhouette. These findings could be consistent with lung atelectasis secondary to obstruction, possibly due to an underlying mass or mucous plugging, and heart failure should be considered as a differential for cardiomegaly. Further diagnostic evaluation and correlation with clinical findings are recommended.
+Instruction	- Enlarged Cardiomediastinum is observed. - Cardiomegaly is present. - Evidence of Lung Opacity is seen. - Extensive consolidation is apparent. - There is Pleural Effusion. - Support devices in the form of a central venous catheter are noted. - No definite pneumothorax, pleural lesions, or fractures are identified.	- Cardiomegaly with associated enlargement of the cardiomediastinum. - Significant lung opacity indicating consolidation, likely due to an infectious or inflammatory process, necessitating further clinical correlation. - Pleural effusion is present. - Central venous catheter in situ. - Absence of pneumothorax or significant pleural disease.
CoT	The cardiomediastinal silhouette is enlarged due to cardiomegaly. There are findings suggesting the presence of pulmonary edema, as evidenced by the perihilar alveolar opacities bilaterally, which may extend to the periphery. No evidence of atelectasis. There is a presence of pleural effusion and support devices, including endotracheal tube above the carina and a gastric tube in the stomach. No lung masses or nodules are identified. No definite pneumothorax or pneumoperitoneum.	Cardiomegaly with signs of pulmonary edema and pleural effusion. Supportive devices in situ. No evidence of atelectasis, pneumothorax, or acute bony injury.
Few-shot	AP supine and lateral decubitus views of the chest demonstrate extensive consolidation involving the right hemithorax with associated volume loss. Evidence of air bronchograms within the consolidation suggests an alveolar filling process, such as pneumonia. There is near-complete opacification of the right lung, with the trachea deviated towards the right side, indicative of volume loss. No visible pneumothorax or significant pleural effusion is noted on the limited view available. The left lung is hyperinflated, likely compensatory. There is a loss of definition of the right heart border and diaphragm silhouette in keeping with the adjacent consolidation. The left hemidiaphragm and heart borders are normal. Osseous structures appear intact but are poorly visualized due to overlying opacity.	Extensive right lung consolidation with volume loss, likely representing a severe pneumonia process. No clear evidence of pleural effusion or pneumothorax on the available projections. Compensatory hyperinflation of the left lung. Clinical correlation and possibly further imaging, such as a CT scan, are recommended for a comprehensive assessment.

Table 23: Comparison of generated reports across different prompting strategies for one study.

Thanks for participating in our human evaluation study! Feel free to reach me at ▨▨▨▨▨▨▨▨▨▨ if you encounter any issue or any questions in the process.

To begin, please register at https://physionet.org/content/mimic-cxr/2.0.0/ and sign the data agreement before the study.

You will be provided with a zipped folder containing an Excel sheet **reader_study_{YOUR_NAME}.csv**, which is the main file you will work on, accompanied by chest X-ray images. If you are a Windows user, no additional action is required. However, if you are using a MacBook, please upload the entire folder to OneDrive and open the Excel sheet from there.

We would like you to complete the rating for 50 patient cases. Each case will include a chest x-ray image, and three reports generated by different methods. ***Please note that the reports we provided are only the impression section.***

Please simulate the real clinical workflow, and give your ratings to the following dimensions:
1. First, take a look at the chest x-ray, and provide your decision on whether each of the reports (impression section) are clinically usable or not, as you would in real practice. (1 means usable and 0 means not usable).

And then, please use likert scale to evaluate each of them in terms of
2. Clinical Efficacy -- Diagnostic Accuracy (Likert 1-5)
   This dimension evaluates how accurate the report is in diagnosing the patient's condition based on the provided chest X-ray image.
3. Clinical Efficacy -- Completeness (Likert 1-5)
   This dimension assesses whether the report covers all relevant clinical findings and provides a comprehensive summary of the patient's condition.
4. Lexical Metrics -- Clarity/Readability (Likert 1-5)
   This dimension evaluates the linguistic quality of the report, focusing on how clear, concise, and easily understandable the text is.

5 is the best score and 1 is the lowest score.

A few notes:
1. Study might contain multiple images. Please click the link_1, link_2, … to view them.
2. Some reports might have masked measurements (xxx cm), and dates, doctor names. Those are de-identified information, please do not consider them as errors.
3. If a report has mention of prior study, please ignore that part and provide your rating only based on the current study's information.

Additionally, please feel free to leave any free-form notes or comments regarding each case. Once you have completed the evaluation for all 50 cases, please return only the Excel sheet to ▨▨▨▨▨▨▨▨▨▨.

Figure 8: Human reader study instructions.

E   Prompts

Table 24: Prompt 1.1 Basic generation: direct report generation based on chest X-ray images.

System	You are a professional chest radiologist that reads chest X-ray image(s).
User	Write a report that contains only the FINDINGS and IMPRESSION sections based on the attached images. Provide only your generated report, without any additional explanation and special format. Your answer is for reference only and is not used for actual diagnosis.

Table 25: Prompt 1.2 Indication enhancement: providing the indication section.

System	You are a professional chest radiologist that reads chest X-ray image(s).
User	Below is INDICATION related to chest X-ray images. INDICATION: { } Write a report that contains only the FINDINGS and IMPRESSION sections based on the attached images and INDICATION. Provide only your generated report, without any additional explanation and special format. Your answer is for reference only and is not used for actual diagnosis.

Table 26: Prompt 1.3 Instruction enhancement: providing information on medical condition labels.

System	You are a professional chest radiologist that reads chest X-ray image(s).
User	Below is an observation plan consisting of 14 conditions: "No Finding", "Enlarged Cardiomediastinum", "Cardiomegaly", "Lung Lesion", "Lung Opacity", "Edema", "Consolidation", "Pneumonia", "Atelectasis", "Pneumothorax", "Pleural Effusion", "Pleural Other", "Fracture", "Support Devices". Based on attached images, assign labels for each condition except "No Finding": "1", "0", "-1", "2". It is noted that "No Finding" is either "2" or "1". These labels have the following interpretation: 1 - The observation was clearly present on the chest X-ray image. 0 - The observation was absent on the chest X-ray image and was mentioned as negative. -1 - The observation was unclear if it exists. 2 - The observation was absent but not explicitly mentioned. Based on labels you choose for each condition, write a report that contains only the FINDINGS and IMPRESSION sections. Don't return any of your assigned labels. Provide only your generated report, without any additional explanation and special format. Your answer is for reference only and is not used for actual diagnosis.

Table 27: Prompt 1.4 Chain-of-Thought: step 1 - medical condition labeling; step 2 - report synthesis.

System	You are a professional chest radiologist that reads chest X-ray image(s).
User	Below is an observation plan consisting of 14 conditions: "No Finding", "Enlarged Cardiomediastinum", "Cardiomegaly", "Lung Lesion", "Lung Opacity", "Edema", "Consolidation", "Pneumonia", "Atelectasis", "Pneumothorax", "Pleural Effusion", "Pleural Other", "Fracture", "Support Devices".

Based on attached images, assign labels for each condition except "No Finding": "1", "0", "-1", "2". It is noted that "No Finding" is either "2" or "1". These labels have the following interpretation:
1 - The observation was clearly present on the chest X-ray image.
0 - The observation was absent on the chest X-ray image and was mentioned as negative.
-1 - The observation was unclear if it exists.
2 - The observation was absent but not explicitly mentioned.

The first step is to return one list of your assigned labels. For multiple images, assign the labels based on all images and return only one list of labels for the given 14 conditions.

The second step is to write a report that contains only the FINDINGS and IMPRESSION sections based on labels you choose for each condition.

Your answer is for reference only and is not used for actual diagnosis. Strictly follow the format below to provide your output.

<LABEL>
[
("No Finding", "1"|"2"),
("Enlarged Cardiomediastinum", "0"|"1"|"2"|"-1"),
("Cardiomegaly", "0"|"1"|"2"|"-1"),
("Lung Lesion", "0"|"1"|"2"|"-1"),
("Lung Opacity", "0"|"1"|"2"|"-1"),
("Edema", "0"|"1"|"2"|"-1"),
("Consolidation", "0"|"1"|"2"|"-1"),
("Pneumonia", "0"|"1"|"2"|"-1"),
("Atelectasis", "0"|"1"|"2"|"-1"),
("Pneumothorax", "0"|"1"|"2"|"-1"),
("Pleural Effusion", "0"|"1"|"2"|"-1"),
("Pleural Other", "0"|"1"|"2"|"-1"),
("Fracture", "0"|"1"|"2"|"-1"),
("Support Devices", "0"|"1"|"2"|"-1")
]
</LABEL>
<REPORT>
FINDINGS: <findings>
IMPRESSION: <impression>
</REPORT>

Table 28: Prompt 1.5 Few-shot: few-shot in-context learning given a few examples (MIMIC).

System	You are a professional chest radiologist that reads chest X-ray image(s).
User	Write a report that contains only the FINDINGS and IMPRESSION sections based on the attached images. Provide only your generated report, without any additional explanation and special format. Your answer is for reference only and is not used for actual diagnosis. [.JPEG] FINDINGS: Single portable view of the chest is compared to previous exam from ___. Enteric tube is seen with tip off the inferior field of view. Left PICC is seen; however, tip is not clearly delineated. Persistent bibasilar effusions and a right pigtail catheter projecting over the lower chest. There is possible right apical pneumothorax. Superiorly, the lungs are clear of consolidation. Cardiac silhouette is within normal limits. Osseous and soft tissue structures are unremarkable. IMPRESSION: No significant interval change with bilateral **pleural effusions** with right pigtail catheter in the lower chest. Possible small right apical pneumothorax. [.JPEG] FINDINGS: Frontal and lateral radiographs of the chest show hyperinflated lungs with flattened diaphragm, consistent with emphysema. Asymmetric opacity in the right middle lobe is concerning for pneumonia. No pleural effusion or pneumothorax is seen. The cardiomediastinal contours are within normal limits aside from a tortuous aorta. IMPRESSION: Right middle lobe opacity concerning for **pneumonia**. [.JPEG] FINDINGS: PA and lateral views of the chest provided. Midline sternotomy wires and mediastinal clips again noted. Suture is again noted in the right lower lung with adjacent rib resection. There is mild scarring in the right lower lung as on prior. There is no focal consolidation, large effusion or pneumothorax. No signs of congestion or edema. The heart remains moderately enlarged. The mediastinal contour is stable. IMPRESSION: Postsurgical changes in the right hemithorax. Mild **cardiomegaly** unchanged. No edema or pneumonia. [.JPEG] FINDINGS: PA and lateral views of the chest provided. Biapical pleural parenchymal scarring noted. No focal consolidation concerning for pneumonia. No effusion or pneumothorax. No signs of congestion or edema. Cardiomediastinal silhouette is stable with an unfolded thoracic aorta and top-normal heart size. Bony structures are intact. IMPRESSION: **No acute findings.** Top-normal heart size. [.JPEG]

Table 29: Prompt 1.5 Few-shot: few-shot in-context learning given a few examples (IU X-RAY).

System	You are a professional chest radiologist that reads chest X-ray image(s).
User	Write a report that contains only the FINDINGS and IMPRESSION sections based on the attached images. Provide only your generated report, without any additional explanation and special format. Your answer is for reference only and is not used for actual diagnosis. [.PNG] FINDINGS: 2 images. Heart size upper limits of normal. Mediastinal contours are maintained. The patient is mildly rotated. There is a small to moderate sized right apical pneumothorax which measures approximately 2.0 cm. No focal airspace consolidation is seen. Left chest is clear. No definite displaced bony injury is seen. Results called XXXX. XXXX XXXX p.m. XXXX, XXXX. IMPRESSION: Small to moderate right apical **pneumothorax**. [.PNG] FINDINGS: The heart is normal in size and contour. There is focal airspace disease in the right middle lobe. There is no pneumothorax or effusion. IMPRESSION: Focal airspace disease in the right middle lobe. This is most concerning for **pneumonia**. Recommend follow up to ensure resolution. [.PNG] FINDINGS: Stable cardiomegaly with vascular prominence without overt edema. No focal airspace disease. No large pleural effusion or pneumothorax. The XXXX are intact. IMPRESSION: Stable **cardiomegaly** without overt pulmonary edema. [.PNG] FINDINGS: Heart is enlarged. There is prominence of the central pulmonary vasculature. Mild diffuse interstitial opacities bilaterally, predominantly in the bases, with no focal consolidation, pleural effusion, or pneumothoraces. XXXX and soft tissues are unremarkable. IMPRESSION: Cardiomegaly with pulmonary interstitial edema and XXXX bilateral **pleural effusions**. [.PNG] FINDINGS: The cardiac silhouette and mediastinum size are within normal limits. There is no pulmonary edema. There is no focal consolidation. There are no XXXX of a pleural effusion. There is no evidence of pneumothorax. IMPRESSION: **Normal chest x-XXXX.** [.PNG] FINDINGS: IMPRESSION: **Presumed closure device** at the level of the ligamentum arteriosum. Normal cardiac silhouette and clear lungs, with no evidence of left-to-right shunt. [.PNG]

Table 30: Prompt 2.1 Image reasoning: medical condition labeling from chest X-ray images (2-class).

System	You are a professional chest radiologist that reads chest X-ray image(s).
User	Below is an observation plan consisting of 14 conditions: "No Finding", "Enlarged Cardiomediastinum", "Cardiomegaly", "Lung Lesion", "Lung Opacity", "Edema", "Consolidation", "Pneumonia", "Atelectasis", "Pneumothorax", "Pleural Effusion", "Pleural Other", "Fracture", "Support Devices".

Based on attached images, assign labels for each condition: "1", "0". If the observation was clearly present on the chest X-ray image, assign "1" to the condition. Otherwise, assign "0" to the condition.

For multiple images, assign the labels based on all images and return only one list of labels for the given 14 conditions. Your answer is for reference only and is not used for actual diagnosis. Strictly follow the format below to provide your output.

<LABEL>
[
("No Finding", "0"|"1"),
("Enlarged Cardiomediastinum", "0"|"1"),
("Cardiomegaly", "0"|"1"),
("Lung Lesion", "0"|"1"),
("Lung Opacity", "0"|"1"),
("Edema", "0"|"1"),
("Consolidation", "0"|"1"),
("Pneumonia", "0"|"1"),
("Atelectasis", "0"|"1"),
("Pneumothorax", "0"|"1"),
("Pleural Effusion", "0"|"1"),
("Pleural Other", "0"|"1"),
("Fracture", "0"|"1"),
("Support Devices", "0"|"1")
]
</LABEL>

Table 31: Prompt 2.2 Image reasoning: medical condition labeling from chest X-ray images (4-class).

User	Below is an observation plan consisting of 14 conditions: "No Finding", "Enlarged Cardiomediastinum", "Cardiomegaly", "Lung Lesion", "Lung Opacity", "Edema", "Consolidation", "Pneumonia", "Atelectasis", "Pneumothorax", "Pleural Effusion", "Pleural Other", "Fracture", "Support Devices".
	Based on attached images, assign labels for each condition except "No Finding": "1", "0", "-1", "2". It is noted that "No Finding" is either "2" or "1". These labels have the following interpretation: 1 - The observation was clearly present on the chest X-ray image. 0 - The observation was absent on the chest X-ray image and was mentioned as negative. -1 - The observation was unclear if it exists. 2 - The observation was absent but not explicitly mentioned.
	For multiple images, assign the labels based on all images and return only one list of labels for the given 14 conditions. Your answer is for reference only and is not used for actual diagnosis. Strictly follow the format below to provide your output.
	<LABEL> [("No Finding", "1"|"2"), ("Enlarged Cardiomediastinum", "0"|"1"|"2"|"-1"), ("Cardiomegaly", "0"|"1"|"2"|"-1"), ("Lung Lesion", "0"|"1"|"2"|"-1"), ("Lung Opacity", "0"|"1"|"2"|"-1"), ("Edema", "0"|"1"|"2"|"-1"), ("Consolidation", "0"|"1"|"2"|"-1"), ("Pneumonia", "0"|"1"|"2"|"-1"), ("Atelectasis", "0"|"1"|"2"|"-1"), ("Pneumothorax", "0"|"1"|"2"|"-1"), ("Pleural Effusion", "0"|"1"|"2"|"-1"), ("Pleural Other", "0"|"1"|"2"|"-1"), ("Fracture", "0"|"1"|"2"|"-1"), ("Support Devices", "0"|"1"|"2"|"-1")] </LABEL>

Table 32: Prompt 3.1 Report synthesis: report generation using provided positive and negative conditions.

System	You are a professional chest radiologist that reads chest X-ray image(s).
User	Below is a given observation plan: <LABEL> Positive Conditions: {} Negative Conditions: {} </LABEL> Write a report that contains only the FINDINGS and IMPRESSION sections based on given labels rather than images. For positive conditions, you should clearly mention it in the report. For negative conditions, you should clearly mention in the report that there is no clear evidence of this condition. You should not mention any other conditions not listed above. Your answer is for reference only and is not used for actual diagnosis. Strictly follow the format below to provide your output. <REPORT> FINDINGS: <findings> IMPRESSION: <impression> </REPORT>

Table 33: Prompt of finetuned LLaMA-2 report synthesis given groundtruth labels

System	Write a radiology report that includes all given positive labels and negative labels.
User	**Input:** Positive labels: {positive_labels} Negative labels: {negative_labels} **Output:** {output}